

A Planck Vacuum Pilot Model for Inelastic Electron-Proton Scattering

William C. Daywitt

National Institute for Standards and Technology (retired), Boulder, Colorado. E-mail: wcdawitt@me.com

This paper describes the scattering of an incident electron from a proton initially at rest, under the assumptions: that the structureless electron interacts directly with the proton and its structure; that the energy and “size” of the electron are determined by its de Broglie radii; and that the shape of the inelastic scattering curve depends upon how deeply the electron core penetrates the proton structure. Deep inelastic scattering ends when the electron is small enough (energetic enough) to penetrate and destroy the proton core and its derived mass.

1 Introduction

The current theory describing electron-proton (e-p) scattering is the Standard Model theory, where the incident electron interacts with the proton via the exchange of a single virtual photon [1, p. 160]. The present paper offers an alternative theory that is based on the emerging Planck vacuum (PV) theory, where the electron interacts directly with the proton [2–5].

In the PV theory both the electron and proton particles are assumed to possess an invisible (vacuum) substructure, while in addition the proton possesses a visible free-space structure due to its positive charge acting on the degenerate PV quasi-continuum (Appendix A). The particle/PV forces and potentials, and their corresponding Compton and de Broglie radii, are associated with this vacuum substructure. The term “structure” by itself refers in what follows exclusively to the free-space proton structure.

2 Electron energy and size

The electron core ($-e_*$, m_e) exerts the two-term coupling force

$$\frac{(-e_*)(-e_*)}{r^2} - \frac{m_e c^2}{r} \quad (1)$$

on the PV state, where the first ($-e_*$) belongs to the electron and the second ($-e_*$) to the separate Planck particles making up the PV continuum. This force difference vanishes

$$\frac{e_*^2}{r_e^2} - \frac{m_e c^2}{r_e} = 0 \quad (2)$$

at the electron Compton radius $r_e (= e_*^2/m_e c^2)$. Treating this vanishing force as a Lorentz invariant constant then leads to the important Compton-(de Broglie) relations for the electron [6]

$$r_e \cdot m_e c^2 = r_d \cdot cp = r_L \cdot E = e_*^2 \quad (= c\hbar) \quad (3)$$

where $p (= m_e \gamma v)$ and $E (= m_e \gamma c^2)$ are the relativistic momentum and energy of the electron, and e_* is the massless bare charge. The radii $r_d (= r_e/\beta\gamma)$ and $r_L (= r_e/\gamma)$ are the electron de Broglie radii in the space and time directions on the Minkowski space-time diagram, where $\beta = v/c < 1$ and $\gamma = 1/\sqrt{1-\beta^2}$.

From (3) the size of the electron is taken to be the de Broglie radii

$$r_d = \frac{r_e}{\beta\gamma} \approx \frac{r_e}{\gamma} = r_L \quad (4)$$

where the approximation applies to the high energy ($\beta \approx 1$) calculations of the present paper. With (4) inserted into (3),

$$cp = \frac{e_*^2}{r_d} \approx \frac{e_*^2}{r_L} = E \quad (5)$$

leading to

$$E = cp = \frac{e_*^2}{r_d} \quad (6)$$

Thus to reduce the electron size to the proton Compton radius ($r_d = r_p$) requires an electron energy equal to $E = e_*^2/r_p$.

The comparisons to follow utilize

$$E = \frac{e_*^2}{r_d} = \frac{e_*^2 r_p}{r_p r_d} = m_p c^2 \frac{r_p}{r_d} \quad (7)$$

to convert electron energies to r_d/r_p ratios. The Lorentz invariance of (2) ensures that equations (3) and (7) apply in any inertial reference frame.

3 Proton structure

The proton substructure arises from the two-term coupling force [7]

$$\frac{(e_*)(-e_*)}{r^2} + \frac{m_p c^2}{r} \quad (8)$$

the proton core (e_* , m_p) exerts on the PV state, where the force vanishes at the proton Compton radius $r_p (= e_*^2/m_p c^2)$.

The proton also possesses a free-space structure (in contradistinction to the electron) in the form of a spherical rest-frame “collar” surrounding the proton core (Appendix A). This collar may affect the formation of the proton de Broglie radii; if, indeed, these radii even exist for the proton. Either way, the following scattering calculations employ only the proton Compton radius from the vanishing of (8).

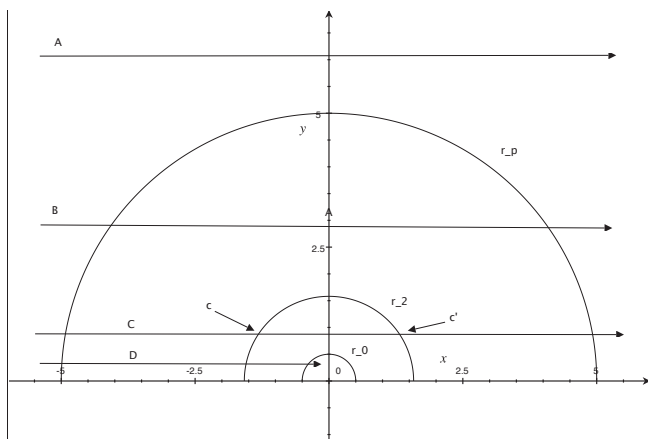


Fig. 1: A highly schematic cross section of the proton structure and four electron-core “trajectories”. The radii r_p and $r_2 (= r_p/3.15)$ represent respectively the proton Compton radius of the substructure and the outer radius of the free-space proton structure.

4 e-p scattering

A highly schematic diagram of the proton cross section is presented in Fig. 1, where r_p is the substructure Compton radius for reference, $r_2 (= r_p/3.15)$ is the outer radius of the proton structure on whose surface resides the apparent charge e of the proton, and r_0 is the radius of the proton core. The latter radius is assumed to be no larger than $r_p/39000$ [7]. Also shown are four electron-core “trajectories” A, B, C, and D, where A and B are propagating in free space and thus represent two elastic e-p scatterings.

Trajectory C ($r_0 < r_d < r_2$) goes through the proton structure, where the electron continuously loses energy (due to excitations of that structure) between its entry and exit points c and c' . Furthermore, since the electron possesses a de Broglie radius (with a corresponding de Broglie wavelength $2\pi r_d$), it exhibits a wave-like nature throughout the trajectory. This wave-like nature, and the finite length ($c-c'$) of the traversed section, produce a resonance within the measured scattering data.

Finally, when the electron energy is great enough ($r_d \ll r_0$) to allow the electron core to penetrate the proton core, this highly energized electron destroys the proton core, leading to the destruction of the proton mass and Compton radius, with a resulting hadron debris field (see Fig. 8.13 in [1, p. 199]).

Fig. 2 shows the experimental scattering data for a beam of 4.879 GeV electrons ($r_d = r_p/5.2$ in (7)) from a proton at rest. The elastic peak at the far right of the figure is represented by B in Fig. 1 with $r_d = r_2$. (This elastic peak is shifted down from the incident electron energy 4.879 GeV to approximately 4.55 GeV ($r_d = r_p/4.9$) by recoil effects.) From the far right to approximately 2.9 GeV on the left the scattering is represented by C in Fig. 1, where the destruction of the proton core has not yet taken place. The three inelastic

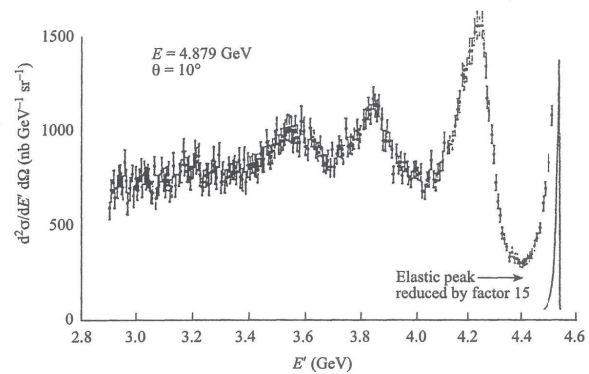


Fig. 2: Elastic and inelastic electron scattering from protons, where E' represents the energy of the scattered electron [9, p. 14] [10]. The scattering angle is 10° . Electron loss increases from right to left.

resonance peaks from left to right in the figure correspond to $r_d \approx r_p/(3.8, 4.1, 4.5)$ from (7).

Fig. 3 shows a repetition of Fig. 2 in a different format, for various scattering angles of the electron. Once more, the destruction of the proton core has not taken place, but the idea of the resonance scattering in the second and fourth paragraphs above is reinforced by the set of five three-peaked curves in the figure. The curves become monotonic when the trajectory between c and c' is deep enough to prevent constructive and destructive interference between reflections at c and c' . Furthermore, when the trajectory is deeper still, D ($r_d \leq r_0$), the electron core will scatter off the proton core.

Again, the proton core is destroyed when $E \gg m_p c^2$ ($r_d \ll r_0$). In this case the incident electron energy is sufficient to overcome the loss sustained in crossing the structure interval ($r_2 - r_0 \approx r_2$) to penetrate the proton core.

Appendix A: Structure

This appendix is a brief review of why the proton is structured and the electron is not [7].

The electron and proton are assumed to exert the two coupling forces

$$F(r) = \pm \left(\frac{e_*^2}{r^2} - \frac{mc^2}{r} \right) \quad (A1)$$

on the PV state, where the plus and minus signs refer to the electron and proton respectively. In effect the negative charge of the electron core ($-e_*, m_e$) in (1) repels the negative PV charges ($-e_*$) away from this core; while the positive charge in the proton core (e_*, m_p) attracts the PV charges. These oppositely charged Coulomb forces (the first terms in (A1)), close to their respective cores, are the fundamental cause of the structureless electron and the structured proton.

The potential energies associated with (A1) are defined by [7]

$$V(r) - V_0 = \int_{0^+}^r F(r') dr' \quad \text{with} \quad V(r_c) = 0 \quad (A2)$$

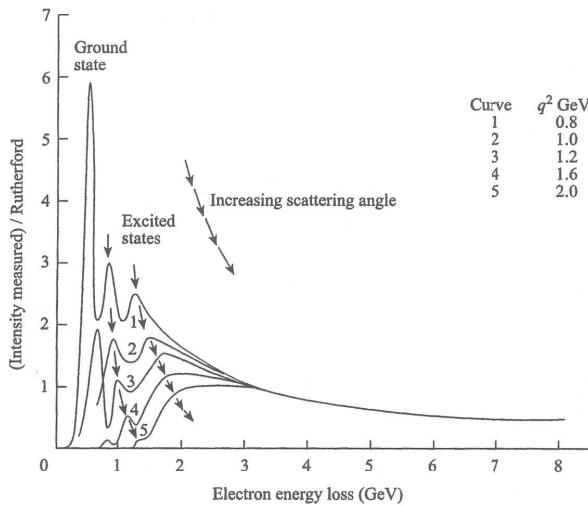


Fig. 3: Inelastic e-p scattering as a function of electron scattering angle [9, p. 17] [11]. Electron loss increases from left to right

where $r_c (= e_*^2/mc^2)$ is the Compton radius of either particle and the 0^+ accounts for the finite (but small) size of the cores. This definition leads to

$$V_p(r) \geq 0 \quad \text{and} \quad V_e(r) \leq 0 \quad (\text{A3})$$

where V_p and V_e are the proton/ and electron/PV coupling potentials.

It is shown in the Klein paradox [8, p. 127] that a sufficiently strong positive potential acting on the vacuum state can force a portion of that state into free space, where that part of the vacuum can then be attacked by free-space particles. Thus the positive and negative potentials in (A3) imply that the proton core, but not the electron core, forces a small spherical (in the core's rest frame) portion of the vacuum into the free space around the proton core. *This free-space vacuum "collar" is identified in the PV theory as the proton structure.* Furthermore, this structure leads to an apparent spread in the charge e_* of the proton core (Appendix B).

Appendix B: Charge spread

The polarization of the proton structure by the proton core leads to an apparent spread of the proton charge that is roughly expressed in the proton electric field as

$$E_p(r) = \frac{e(r)}{r^2} \quad (\text{B1})$$

where the spread is

$$e(r) = \begin{cases} e_* & , r < r_0 \\ < e_* & , r_0 < r < r_2 \\ e = \alpha^{1/2} e_* & , r_2 \leq r \end{cases} \quad (\text{B2})$$

$r_2 = r_p/3.15$, and $\alpha (\approx 1/137)$ is the fine structure constant. The radius r_2 defines the outer extent of the proton structure.

An important characteristic of this result is the large charge gradient

$$\frac{\Delta e}{\Delta r} = \frac{e - e_*}{r_2 - r_0} \approx -\frac{e_*(1 - \sqrt{\alpha})}{r_2} \approx -\frac{0.92e_*}{r_2} \quad (\text{B3})$$

between the core charge e_* and the observed proton charge e at r_2 . This result explains a similar gradient in the QED spread depicted in Fig. 11.6 of [9, p. 319].

Submitted on June 11, 2015 / Accepted on July 2, 2015

References

1. Thomson M. Modern Particle Physics. McGraw-Hill Book Company, U.S.A., 2013.
2. Daywitt W.C. The Planck Vacuum. *Progress in Physics*, 2009, v. 5 (1), 20. See also www.planckvacuum.com.
3. Daywitt W.C. The Source of the Quantum Vacuum. *Progress in Physics*, 2009, v. 5 (1), 27.
4. Daywitt W.C. The Electron and Proton Planck-Vacuum Coupling Forces and the Dirac Equation. *Progress in Physics*, 2014, v. 10, 114.
5. Daywitt W.C. The Strong and Weak Forces and their Relationship to the Dirac Particles and the Vacuum State. *Progress in Physics*, 2015, v. 11, 18.
6. Daywitt W.C. The de Broglie Relations Derived from the Electron and Proton Coupling to the Planck Vacuum State. *Progress in Physics*, 2015, v. 11 (2), 189.
7. Daywitt W.C. The Structured Proton and the Structureless Electron as Viewed in the Planck Vacuum Theory. *Progress in Physics*, 2015, v. 11 (2), 117.
8. Gingrich D.M. Practical Quantum Electrodynamics. CRC, The Taylor & Francis Group, Boca Raton, 2006.
9. Aitchison I.J.R., Hey A.J.G. Gauge Theories in Particle Physics, Vol. 1. Taylor & Francis, New York, London, 2003.
10. Bartel W.B. *et al.* Electroproduction of Pions Near the $\Delta 1236$ Isobar and the Form Factor $G_M^*(q^2)$ of the $(\gamma N \Delta)$ -Vertex. *Phys. Lett.*, 1968, v. 28B, 148.
11. Perkins D. Introduction to High Energy Physics, 1st ed. Addison Wesley Publishing, 1972.